Springer

Journal of
Mechanical
Science and
Technology

Journal of Mechanical Science and Technology 22 (2008) 41~49

www.springerlink.com/content/1738-494x

Discrete thickness optimization of an automobile body by using the continuous-variable-based method

Gang-Won Jang[1,*], Young-Min Choi[2] and Gyoo-Jae Choi[1]

[1]*School of Mechanical Engineering, Kunsan National University, Kunsan, Chonbuk 573-701, Korea*
[2]*Tokyo Electron Korea Ltd., Youngtong, Suwon, Gyeonggi 443-766, Korea*

(Manuscript Received March 27, 2007; Revised July 5, 2007; Accepted July 24, 2007)

Abstract

Design optimization of an automobile body for dynamic stiffness improvement is presented. The thicknesses of plates consisting of a monocoque body of an automobile are employed as design variables for optimization whose objective is to increase the first torsional and bending natural frequencies. By allotting one design variable to each plate of the body, compared to previous works based on element-wise design variables, the design space of optimization can be reduced to a large extent. Because the present optimization is based on continuous-variable-based algorithms, considering manufacturability of the optimized result, the converged values of plate thicknesses should be approximated to commercially available discrete values. A new straightforward thickness discretization scheme considering design sensitivities and employing a subsequent reduced optimization problem is proposed. The validity of the proposed thickness discretization scheme is verified through numerical experiments.

Keywords: Thickness optimization; Discrete optimization; Natural frequency maximization; BIW; Manufacturability

1. Introduction

The fierce competition within the car industry by globalization of the markets requires manufacturers to shorten their development time for new models. To this end, CAE-based structural optimization techniques have been actively utilized to design lightweight parts with high static and dynamic performance. For example, Chiandussi et al. [1] used topology optimization to reduce the weight of a sub-frame for a suspension system. Chen et al. [2] optimized the shape of a fuel tank, and Leiva et al. [3] introduced size optimization to determine the location of weld points. Hwang et al. [4] designed a rear-view mirror with enhanced dynamic performance by using shape optimization whose design parameters are determined by the Taguchi method. Kim et al. [5] improved the fatigue life of a lower control arm by using the design of experiment approach.

In this work, we apply CAE-based optimization to increase the overall dynamic performance of an automobile body. The thicknesses of the plates consisting of the monocoque body of an automobile are parameterized with design variables for optimization, and the design objective is set to maximize the first torsional and bending natural frequencies. The optimization is performed for a car model that has already been produced. The thicknesses of the plates are increased or decreased with respect to the values of design variables, so an optimization algorithm will reinforce the plates which have a large influence on the frequency increase and vice versa.

The optimization of a full car model for dynamic performance increase was performed by Wang et al. [6], who discretized the BIW (body-in-white) model of the Porsche 928 with over 34,000 finite elements. They allotted one design variable for each finite element and proposed the reinforcement of the automo-

*Corresponding author. Tel.: +82 63 469 4725, Fax.: +82 63 469 4727
E-mail address: gangwon@kunsan.ac.kr
DOI 10.1007/s12206-007-1005-x

bile body by performing topology and thickness optimizations. For topology optimization, they added a new layer of elements on the existing elements and endowed the added elements with design variables. Also, for thickness optimization, they directly treated thicknesses as design variables. However, the design space in their approach was very big with many design variables and accordingly the numerical cost was tremendous. Because the optimization in Reference [6] used continuous design variables, the optimized thickness was not discretely calculated, which is not favorable for production of the optimized body.

In this work, the design variables are allotted to each plate of a monocoque body, and thus the number of design variables and design space can be significantly reduced compared to the approach in Reference [6]. The proposed thickness optimization is performed based on a continuous variable design space. Thus gradient-based fast optimization algorithms are employed as the optimizer. However, because commercially available plate thicknesses for the automobile body are discrete, optimized thicknesses should be approximated to the discrete values to ensure manufacturability. To discretely optimize the plate thicknesses, non-gradient-based algorithms such as the genetic algorithm [7], the particle swarm method [8] and the branch-and-bound method [9] might be introduced. However, the computational cost for such optimizations would be enormous especially for full car models of this work.

We propose a new thickness discretization approach which minimizes the performance change of the continuous-thickness-based optimization results. Because the present problem deals with natural frequencies as performance measures for optimization, unlike static cases, design sensitivity is not always positive with respect to the increase of the plate thickness. Thus, if some final sensitivities of the continuous-thickness-based optimization are negative, their corresponding intermediate thicknesses are easily discretized to smaller available discrete thicknesses. By doing this intuitive post-process, the mass of the optimized structure can be efficiently reduced without affecting system performance. For thicknesses having positive design sensitivities, a reduced optimization problem is formulated for further discretization. In the reduced problem, an explicit penalty term for intermediate thicknesses is imposed on the design objective.

The commercial software ANSYS [10] and DOT [11] are used for the finite element analysis and optimization, respectively.

2. Formulation of thickness optimization

The BIW model of a car that is used for optimization in this work is illustrated in Fig. 1(a). The model consists of 51 steel plate parts, among which 19 parts in the middle rear region of the car are set as design variables. Fig. 1(b) shows the design variables. The total mass of the model is 251.4 kg.

Fig. 2 shows modal analysis results of the model in Fig. 1 conducted by using the ANSYS shell 63 element. The first torsional mode is found to be the 8th mode with its natural frequency 22.7 Hz and the first bending mode is the 11th mode with its natural frequency 33.5 Hz.

The optimization for increasing torsional and bending frequencies of the BIW model is formulated as

$$\underset{\boldsymbol{\rho}\in\mathbb{R}^N}{\text{Maxmize}} \quad F = w\frac{f_{\mathrm{T}}(\boldsymbol{\rho})}{f_{\mathrm{T}}^0} + (1-w)\frac{f_{\mathrm{B}}(\boldsymbol{\rho})}{f_{\mathrm{B}}^0} \tag{1a}$$

$$\text{Subject to} \quad G = \Sigma m_i - M_0 < 0 \qquad 0 \le \rho_i \le 1 \quad (i = 1,2,3,...,N), \tag{1b}$$

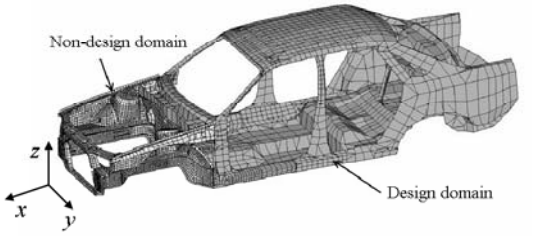

(a) Non-design domain and design domain

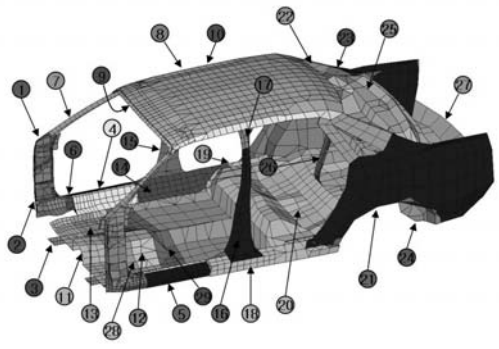

(b) Design variables in the design domain

Fig. 1. Body-in-white model of an automobile

(a) First torsional mode (f_T =22.7 Hz)

(b) First bending mode (f_B = 33.5 Hz)

Fig. 2. Modal analysis results

where f_{T} and f_{B} are the first torsional and bending frequencies, respectively. In Eq. (1a), $\boldsymbol{\rho} \in \mathbb{R}^N$ denotes the design variable vector, which is parameterized with plate thickness. In the equation, the superscript 0 denotes the values calculated from the initial model. The contribution of each frequency to the objective is controlled by adjusting the weight parameter w $(0 \le w \le 1)$. The design constraint in (1b) is imposed on total mass of the model not to exceed the prescribed mass M_0, and m_i in (1b) denotes the mass of the plate which is linked with ρ_i.

The parameterization of the design variable with the plate thickness is defined as

$$t_i = (\alpha + \beta \cdot \rho_i) t_i^0 \quad i = 1,2,3,...,N, \tag{2}$$

where t_i^0 is the thickness of the plate *i* of the original model, and α and β are parameters to express the maximum and minimum plate thickness for optimization, respectively. In this work, the parameters are set as $\alpha = 0.8$ and $\beta = 1.2$, so plate thicknesses are varied 80-200% according to the values of their design variables.

As an analysis module ANSYS is employed by using its programming language form APDL (ANSYS Parametric Design Language), and the sequential quadratic programming of DOT [11] is used for optimization. The design sensitivities are calculated by using the forward finite difference approach because explicit forms of element stiffness matrices or mass matrices are not available for the commercial analysis software.

Table 1. Optimized first torsional frequencies $(w = 1)$.

Mass constraint [kg]	Added mass	Frequency [Hz]	Frequency Increase
254.0	2.6	28.8	6.1
259.0	7.6	29.3	6.6

3. Optimization results with continuous thicknesses

3.1 Maximization of the torsional natural frequency

By setting $w = 1$ in (1a), the first torsional natural frequency is considered as the only design objective. The optimization is performed for two cases: 1) 1% mass increase (2.6 kg) and 2) 3% mass increase (7.6 kg). Although the torsional mode was found as the 8th mode in the original model, there exists high possibility of mode sequence change during optimization. Therefore, the mode of interest should be tracked during optimization. We use the MAC-based mode-tracking method proposed by Kim and Kim [12]. In [12], the MAC (modal assurance criterion) between two different modes is defined as

$$\mathbf{MAC}(\boldsymbol{\Phi}_A, \boldsymbol{\Phi}_B) = \frac{\left|\boldsymbol{\Phi}_A^T \boldsymbol{\Phi}_B\right|}{\left(\boldsymbol{\Phi}_A^T \boldsymbol{\Phi}_A\right)\left(\boldsymbol{\Phi}_B^T \boldsymbol{\Phi}_B\right)}, \tag{3}$$

where $\boldsymbol{\Phi}_A$ and $\boldsymbol{\Phi}_B$ denote modal vectors of mode A and mode B, respectively. The MAC value is obtained as $0 \le \mathbf{MAC} \le 1$. If $\mathbf{MAC} = 1$, it indicates that the two modes are exactly equal to each other.

Table 1 shows the maximized torsional natural frequencies for two mass constraint conditions after optimization. While the mass increases only 1 or 3%, the frequency increase rate is optimized more than 26%. This means that the mass of the plates having small contribution to the increase of torsional frequency efficiently moves to the plates having large contribution for the frequency increase. In other words, mass decreases during optimization for the plates whose mass increase rates for unit thickness

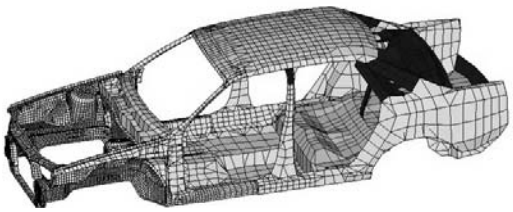

(a)

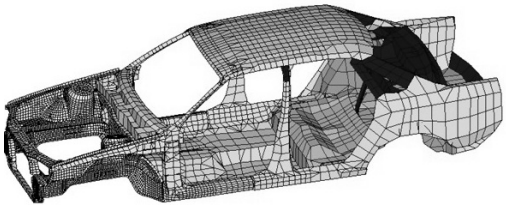

(b)

Fig. 3. First torsional frequency maximization results: (a) 1% added mass, and (b) 3% added mass (: $0.8 < \rho_i \le 1$, : $0.6 < \rho_i \le 0.8$, : $0.4 < \rho_i \le 0.6$, : $0.2 < \rho_i \le 0.4$ and : $0 \le \rho_i \le 0.2$).

Table 2. Optimized thicknesses of the plates for torsional frequency maximization problem with 1% added mass.

i	t_i^0	t_i^{opt}	i	t_i^0	t_i^{opt}
1	1	0.800	16	1.4	1.120
2	1.8	1.440	17	1	1.989
3	0.8	0.640	18	1	0.800
4	1.4	1.120	19	1.4	1.120
5	1	0.800	20	1.2	1.615
6	1.4	1.120	21	1	0.800
7	3	2.401	22	1	1.999
8	2	1.600	23	1	0.800
9	1.4	1.121	24	1	0.833
10	1	0.888	25	1	1.999
11	1.6	1.280	26	1	1.999
12	1.4	1.120	27	1.6	3.199
13	1.4	1.120	28	1	0.800
14	1.4	1.120	29	1.2	0.960
15	1.6	1.280			

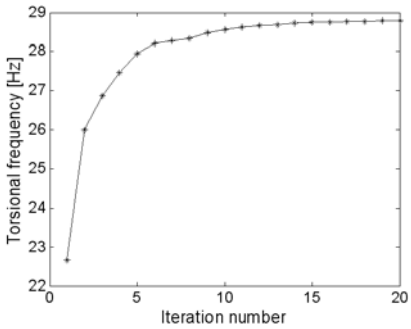

Fig. 4. Objective function history of the torsional frequency maximization problem.

Table 3. Optimized first bending frequencies ($w = 0$) .

Mass constraint [kg]	Added mass	Frequency [Hz]	Frequency increase
254.0	2.6	40.3	6.8
259.0	7.6	41.4	7.9

Table 4. Optimized thicknesses of the plates for bending frequency maximization problem with 1% added mass.

i	t_i^0	t_i^{opt}	i	t_i^0	t_i^{opt}
1	1	2.000	16	1.4	1.120
2	1.8	3.600	17	1	2.000
3	0.8	0.640	18	1	0.800
4	1.4	1.120	19	1.4	1.120
5	1	0.800	20	1.2	0.960
6	1.4	1.120	21	1	0.800
7	3	4.411	22	1	0.877
8	2	1.658	23	1	0.872
9	1.4	2.800	24	1	0.800
10	1	1.931	25	1	1.996
11	1.6	1.280	26	1	0.800
12	1.4	1.120	27	1.6	1.618
13	1.4	2.543	28	1	0.800
14	1.4	1.120	29	1.2	0.960
15	1.6	1.280			

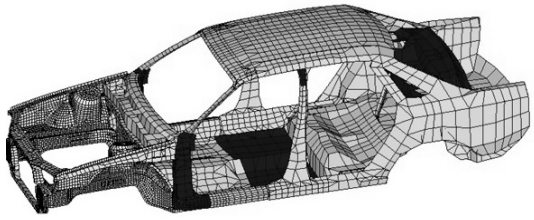

(a)

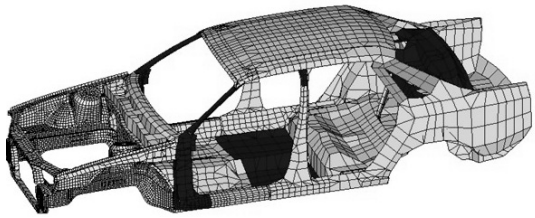

(b)

Fig. 5. First bending frequency maximization results: (a) 1% added mass, and (b) 3% added mass (: $0.8 < \rho_i \le 1$, : $0.6 < \rho_i \le 0.8$, : $0.4 < \rho_i \le 0.6$, : $0.2 < \rho_i \le 0.4$ and : $0 \le \rho_i \le 0.2$).

increase are larger or equal to their stiffness increase rates, and vice versa.

Fig. 3 illustrates thickness changes of the plates after optimization. Reinforcements are mainly found for the plates whose displacements are largely evaluated in the modal vector Fig. of Fig. 2(a). The optimized plate thicknesses for the case of 1% mass increase are listed in Table 2. The proposed thickness optimization formulation is based on continuous real design variables, and thus additional post-process step for approximating optimized thicknesses to available discrete thicknesses are required. This will be discussed in detail in section 4. Fig. 4 shows the history of the torsional natural frequency during optimization.

3.2 Maximization of the bending natural frequency

Next, we consider only the increase of the bending natural frequency ($w = 0$ in (1a)). The results of optimization are listed in Table 3. The frequency increases 6.8Hz and 7.9Hz for 1 and 3% mass increase, respectively. The optimized plate thicknesses for the case of 1% mass increase are listed in Table 4, and also illustrated in Fig. 5. As in the torsional frequency increase problem, thicknesses are mainly increased on the plates whose mode vectors are largely calculated in Fig. 2(b); thicknesses of the plates around A pillar, top region of B pillar, bottom and rear parts are doubly increased.

3.3 Maximization of the torsional and bending natural frequencies

Both the first torsional and bending natural frequencies are considered as the design objective by using $w = 0.5$ in (1a). One mass constraint condition of 1% mass increase is used in the optimization. The results are listed in Table 5, which shows less frequency increase compared to the results of considering either the torsional or bending frequency as the only objective. Nonetheless, a large frequency increase and thus high dynamic stiffness of the optimized body can be obtained compared to the original model.

The mode sequence of the first torsional mode of the optimized model is changed to the 10^{th} from the 8^{th} of the original model and that of the first bending mode is also changed to the 13^{th} from the 11^{th}. Thus, without employing a mode-tracking method such as the MAC [12], it is hard to expect meaningful designs in the proposed optimization problems.

Table 5. Frequency increase results by multi objective topology optimization with 1% mass increase ($w = 0.5$) .

	Initial design [Hz]	Optimized design [Hz]	Frequency increase
Torsional frequency	22.7	28.4	5.7
Bending frequency	33.5	39.2	5.7

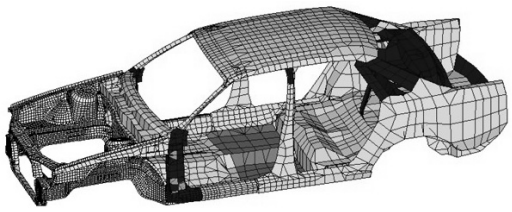

Fig. 6. Thickness optimization result by multi objective optimization with 1% added mass (■: $0.8 < \rho_i \le 1$, ■: $0.6 < \rho_i \le 0.8$, ■: $0.4 < \rho_i \le 0.6$, ■: $0.2 < \rho_i \le 0.4$ and ■: $0 \le \rho_i \le 0.2$).

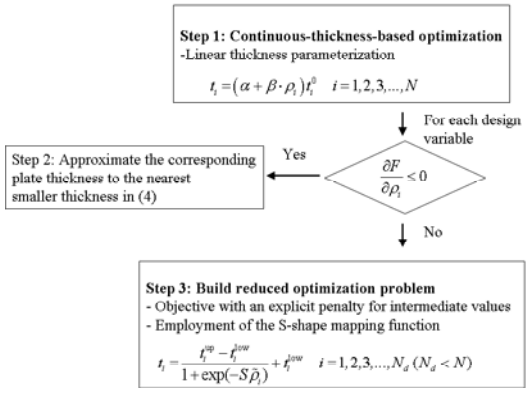

Fig. 7. The proposed thickness discretization scheme.

Fig. 6 illustrates the optimized plate thicknesses. In the figure, the thickness reinforcement patterns in Fig. 3(a) and Fig. 5(a) can be found mixed.

4. Discrete thickness optimization process

The plate thicknesses are optimized based on continuous design variables ρ_i , so their values after optimization are also continuous as in Table 2 and Table 4. However, manufacturing all the plates having arbitrary thickness dimensions in Table 2 or Table 4 involves tremendous cost increase. In this work, the manufacturability issue of optimization is considered by approximating optimized plate thicknesses to the following discrete values:

$$\bar{t}_i \in \{0.6, 0.65, 0.7, 0.8, 0.9, 1.0, 1.2, 1.4, 1.6, 1.8, 2.0, 2.3, 2.6, 3.0\} \text{ [mm]}. \quad (4)$$

In Fig. 7, we propose a straightforward thickness discretization approach based on two subsequent optimizations. The first step in the figure denotes the continuous-thickness-based optimization which is already defined in Eq. (1) and Eq. (2). After Step 1 optimization, thickness discretization can be easily performed for the plates whose optimized thicknesses are almost close to those in (4).

As the second step of the proposed discretization, considering design sensitivities of the optimized result, we can determine discrete values of some intermediate optimized thicknesses. In Fig. 8, we show the sensitivities of the objective and the mass constraint for the optimized result in Fig. 3(a). According to Eq. (2), the sensitivity of the objective F is

$$\frac{\partial F}{\partial \rho_i} = \frac{\partial F}{\partial t_i} \beta t_i^0 . \quad (5)$$

Because βt_i^0 is positive, Eq. (5) means that the sign of $\partial F/\partial t_i$ is always equal to that of $\partial F/\partial \rho_i$. Thus, if the objective sensitivity with respect to a design variable is negative, it indicates that the natural frequencies decrease as the thickness of the corresponding plate increases. Accordingly, for the design variables with $\partial F/\partial \rho_i \le 0$, the corresponding optimized thicknesses should be approximated to their nearest smaller discrete thicknesses in (4) to reduce total mass of the automobile body. For example, if the optimized thickness of a plate is $t_i^{\text{opt}} = 1.18$ m and its objective sensitivity is negative, the discrete thickness is $\bar{t}_i = 1.0$ mm. Also, if $t_i^{\text{opt}} = 2.23$ m and its objective sensitivity is negative, its discrete thickness is $\bar{t}_i = 2.0$ mm. In Fig. 8, the 1st, 2nd, 3rd, 4th, 5th, 6th, 9th, 12th, 13th, 18th, 28th and 29th design variables have negative design sensitivities for the objective and should be approximated to their nearest smaller discrete values.

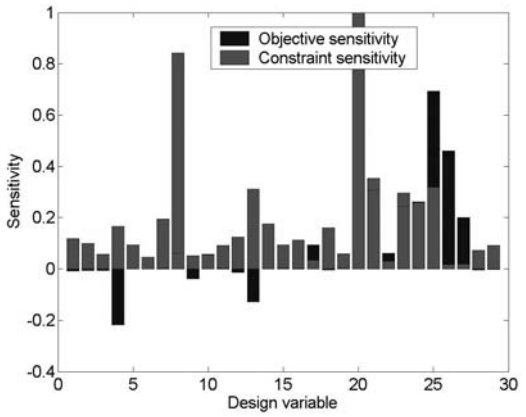

Fig. 8. Sensitivities of the result in Fig. 3(a).

Step 3 in Fig. 7 is given as a reduced optimization problem for the discretization of intermediate optimized thicknesses having positive objective sensitivities:

$$\underset{\tilde{\boldsymbol{\rho}} \in \mathbb{R}^{N_d}}{\text{Maxmize}} \quad \tilde{F} = w\frac{f_{\text{T}}(\tilde{\boldsymbol{\rho}})}{f_{\text{T}}^0} + (1-w)\frac{f_{\text{B}}(\tilde{\boldsymbol{\rho}})}{f_{\text{B}}^0} - \frac{1}{R}\sum_{i=1}^{N}\left(t_i^{\text{up}} - t_i\right)\left(t_i - t_i^{\text{low}}\right) \quad (6a)$$

$$\text{Subject to} \quad G = \Sigma m_i - M_0 < 0, \quad -1 \le \tilde{\rho}_i \le 1 \quad (i = 1, 2, 3, ..., N_d), \quad (6b)$$

and

$$t_i = \frac{t_i^{\text{up}} - t_i^{\text{low}}}{1 + \exp(-10\tilde{\rho}_i)} + t_i^{\text{low}} , \quad (6c)$$

where $\tilde{\boldsymbol{\rho}}$ ($\subset \boldsymbol{\rho}$) is a reduced set of design variables whose objective sensitivities are positive after the Step 1 optimization. Thus, it is obvious that $N_d < N$. In the above, t_i^{up} and t_i^{low} denote the nearest larger and smaller discrete thicknesses of the intermediate thickness t_i, respectively. Note that, to enforce the convergence to discrete values, an explicit penalty term for intermediate thicknesses is imposed on the new objective function in Eq. (6a). The parameter R in Eq. (6a) is a normalization parameter whose value is set to make the penalty term unity at the beginning of the optimization.

In Eq. (6c), the design variable $\tilde{\rho}_i$ is nonlinearly parameterized with the thickness by using the so-called S-shape mapping function illustrated in Fig. 9(a) [13]. Fig. 9(b) shows that the derivative of the mapping function has large values around intermediate design variables. Thus, by using an S-shape mapping function, high sensitivities around intermediate design values are obtained, and accordingly the pushing effect of t_i to t_i^{up} or t_i^{low} can be expected (see Reference [13] for more details.)

Using the proposed discretization scheme, the resulting thicknesses of the continuous-thickness-based

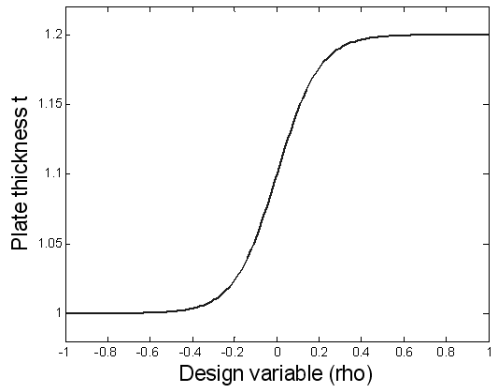

(a)

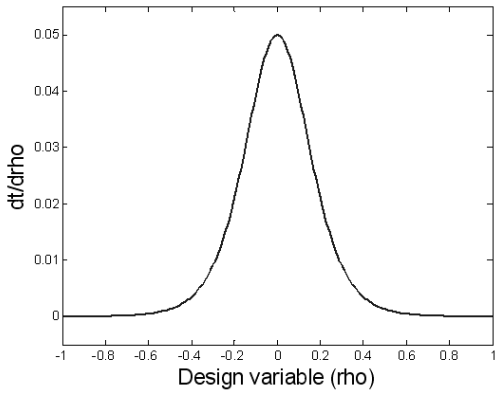

(b)

Fig. 9. (a) S-shape mapping function from $\tilde{\rho}_i$ to t_i and (b) $dt_i/d\tilde{\rho}_i$.

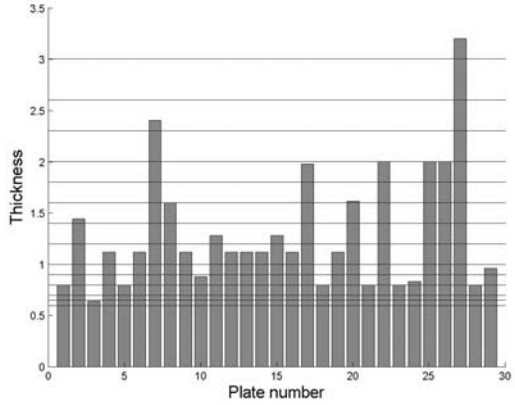

(a)

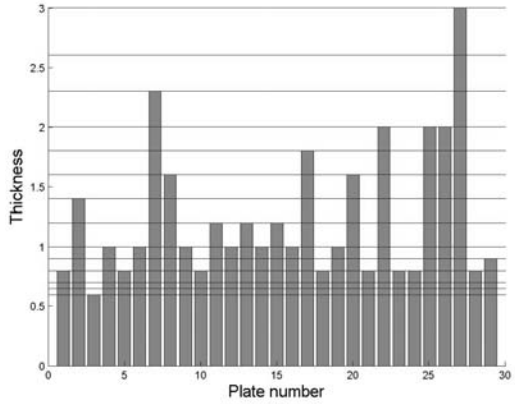

(b)

Fig. 10. Discretization of the optimized thickness results of the torsional frequency maximization problem in Fig. 3(a): (a) optimized thicknesses after the Step 1 optimization, and (b) discretized thicknesses after the Step 3 optimization (horizontal lines denote the discrete thicknesses in (4)).

optimization (or the Step 1 optimization) in Table 2 for torsional frequency maximization with 1% added mass are discretized. Table 6 lists the discretized thicknesses. In the Step 2 column of Table 6, discretized thicknesses belong to one of the following cases. ① A thickness after the Step 1 optimization is nearly close to one of the discrete values in (4). ② The design sensitivity for the objective function is negative and thus the thickness is approximated to its nearest smaller discrete thickness. A total of 19 out of 29 thicknesses are directly discretized through the Step 2 process. The remaining 10 intermediate thicknesses are set as design variables for the reduced optimization problem of Step 3. Because the number of design variables for the reduced problem is smaller than that of the Step 1 optimization, the total computational cost for the optimization does not seriously increase. Fig. 10 shows the discretization effect of the proposed approach; the intermediate thicknesses in Fig. 10(a) are approximated to those in Fig. 10(b). The horizontal lines in Fig. 10 denote the discrete thicknesses in (4). The torsional frequency of the discretely optimized structure is 28.6 Hz. The final mass is 250.2 kg, which is rather decreased from 254.0 kg of the Step 1 result through the discretization.

For the optimized results of the torsional and bending frequency maximization problem in Fig. 6, discretized thicknesses are also calculated and listed in Table 7. Fig. 11 shows the thicknesses before and after the discretization. The final optimized structure has 28.4 Hz for the torsional frequency and 39.6 Hz for the bending frequency and the mass is 251.4 kg. Compared to the initial model, the torsional frequency

Table 6. Optimized thicknesses t_i^{opt} after the Step 1 optimization Eqs. (1) and their discretized values for torsional frequency maximization problem with 1% added mass (In Step2, thicknesses with negative design sensitivities for the objective are underlined).

i	t_i^0	t_i^{opt}	Step2	Step3	i	t_i^0	t_i^{opt}	Step2	Step3
1	1	0.800	0.8	←	16	1.4	1.120		1.0
2	1.8	1.440	1.4	←	17	1	1.976		1.8
3	0.8	0.640	0.6	←	18	1	0.800	0.8	←
4	1.4	1.120	1.0	←	19	1.4	1.120		1.0
5	1	0.800	0.8	←	20	1.2	1.616		1.6
6	1.4	1.120	1.0	←	21	1	0.800	0.8	←
7	3	2.400		2.3	22	1	2.000	2.0	←
8	2	1.600	1.6	←		1	0.800	0.8	←
9	1.4	1.120	1.0	←	24	1	0.834		0.8
10	1	0.879		0.8	25	1	2.000	2.0	←
11	1.6	1.280		1.2	26	1	2.000	2.0	←
12	1.4	1.120	1.0	←	27	1.6	3.199	3.0	←
13	1.4	1.120	1.0	←	28	1	0.800	0.8	←
14	1.4	1.120		1.0	29	1.2	0.960	0.9	←
15	1.6	1.280		1.2					

Table 7. Optimized thicknesses t_i^{opt} after the Step 1 optimization Eqs. (1) and their discretized values for torsional and bending frequency maximization problem with 1% added mass.

i	t_i^0	t_i^{opt}	Step2	Step3	i	t_i^0	t_i^{opt}	Step2	Step3
1	1	1.9860	2.0	←	16	1.4	1.1228		1.2
2	1.8	1.9350		1.8	17	1	1.9868	2.0	←
3	0.8	0.6416		0.65	18	1	0.8020	0.8	←
4	1.4	1.1228		1.0	19	1.4	1.1228		1.0
5	1	0.8020	0.8	←	20	1.2	1.0959		1.0
6	1.4	1.1228		1.0	21	1	0.8020	0.8	←
7	3	2.4060		2.6	22	1	1.6706		1.8
8	2	1.6040	1.6	←	23	1	0.8020	0.8	←
9	1.4	2.7814		2.6	24	1	0.8239		0.9
10	1	1.4485		1.4	25	1	1.9900	2.0	←
11	1.6	1.2832		1.2	26	1	1.9898	2.0	←
12	1.4	1.1228		1.0	27	1.6	3.1708	3.0	←
13	1.4	2.1942		2.3	28	1	0.8020	0.8	←
14	1.4	1.1228		1.2	29	1.2	0.9624		0.9
15	1.6	1.2832		1.4					

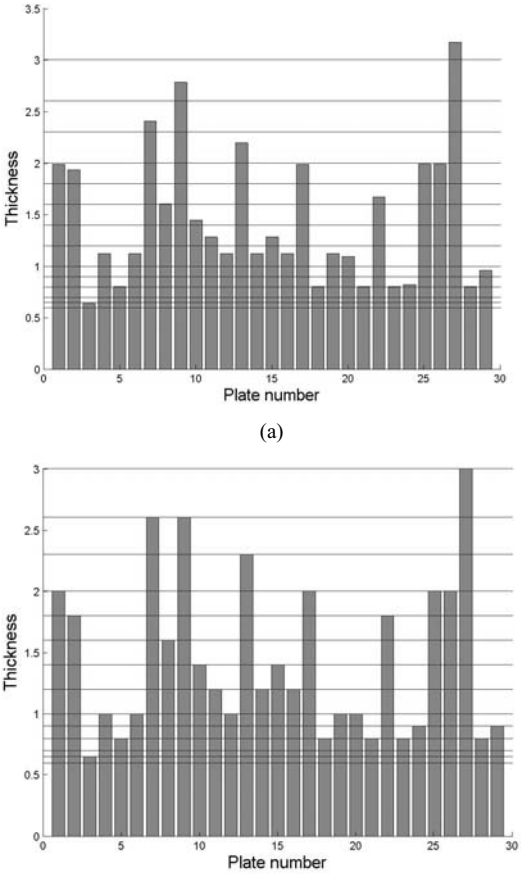

Fig. 11. Discretization of the optimized thickness results of the torsional and bending frequency maximization problem in Fig. 6 (a) optimized thicknesses after the Step 1 optimization, and (b) discretized thicknesses after the Step 3 optimization [horizontal lines denote the discrete thicknesses in (4)].

and the bending frequency of the structure are increased 5.7 Hz and 6.1 Hz, respectively.

5. Conclusions

A torsional and bending frequency maximization problem for the BIW model of an automobile body was presented in this work. Compared to the existing element-wise design variable approach, by allotting design variables onto each plate of the model and linearly parameterizing the design variable with its corresponding plate thickness, the size of the design space could be significantly reduced. A straightforward thickness discretization scheme was newly proposed for increasing manufacturability of the optimized structure. By examining the design sensitivities

of the objective function, some of intermediate thicknesses could be directly discretized. After the intuitive discretization, a reduced optimization problem was reformulated where side constraints for the intermediate thicknesses were limited to their adjacent discrete thicknesses. The parameterization of design variables and the objective function was modified to enforce the convergence of thicknesses to discrete values. The optimized structure showed around 6 Hz frequency increase with less mass than the initial model.

References

[1] G. Chiandussi, I. Gaviglio and A. Ibba, Topology optimization of an automotive component without final volume constraint specification, *Advances in Engineering Software* 35 (2004) 609-617.

[2] C. J. Chen, S. Maire and M. Usman, Improved fuel tank design using optimization, ASME McNu97' Design Optimization with Applications in Industry Symposium, Chicago, USA, (1997).

[3] J. P. Leiva, L. Wang, S. Recek and B. C. Watson, Automobile design using the GENESIS structural optimization program, NAFEMS Advances in Optimization Technologies for Product Design, Chicago, USA. (2001).

[4] K. H. Hwang, K. W. Lee and G. J. Park, Robust optimization of an automobile rearview mirror for vibration reduction, *Struct. Multidisc. Optim.* 21 (2001) 300-308.

[5] M. S. Kim, C. W. Lee, S. Son, H. J. Yim and S. J. Heo, Shape optimization for improving fatigue life of a lower control arm using the experimental design, *Transactions of the KSAE* 11 (3) (2003) 161-166.

[6] L. Wang, P. K. Basu and J. P. Leiva, Automobile body reinforcement by finite element optimization, *Finite Elements in Analysis and Design* 40 (2004) 879-893.

[7] D. E. Goldberg, Genetic Algorithms in Search, Optimization, and Machine Learning, Kluwer Academic Publishers, Boston, MA, (1989).

[8] M. Tayal and B. Wang, Particle swarm optimization for mixed discrete, integer and continuous variables, 10th AIAA/ISSMO Multidisciplinary Analysis and Optimization Conference, Albany, New York, USA, (2004).

[9] O. K. Gupta and A. Ravindran, Branch and bound experiments in convex nonlinear integer programming, *Manage. Sci.* 31 (1985) 1533-1546.

[10] ANSYS, ANSYS Advanced Analysis Technique Guide, (2006).

[11] Vanderplaats Research & Development, Inc., DOT Users Manual, (1999).

[12] T. S. Kim and Y. Y. Kim, Mac-based mode-tracking in structural topology optimization, *Computers and Structures* 74 (2000) 375-383.

[13] G. H. Yoon and Y. Y. Kim, The role of S-shaped mapping functions in the SIMP approach for topology optimization, *KSME Int. J.* 15 (2003) 1496-1506.